Spring 1-1-2017

Stabilized Conservative Level Set Method with Adaptive Wavelet-Based Mesh Refinement

Navid Shervani-Tabar
University of Colorado at Boulder, navidst@colorado.edu

Stabilized Conservative Level Set Method with Adaptive Wavelet-based Mesh Refinement

by

N. Shervani-Tabar

B.S., University of Tabriz, 2014

A thesis submitted to the

Faculty of the Graduate School of the

University of Colorado in partial fulfillment

of the requirements for the degree of

Master of Science

Department of Mechanical Engineering

2017

This thesis entitled:
Stabilized Conservative Level Set Method with Adaptive Wavelet-based Mesh Refinement
written by N. Shervani-Tabar
has been approved for the Department of Mechanical Engineering

Prof. Oleg V. Vasilyev

Prof. John A. Evans

Prof. Michael P. Hannigan

Prof. Peter E. Hamlington

Date

The final copy of this thesis has been examined by the signatories, and we find that both the content and the form meet acceptable presentation standards of scholarly work in the above mentioned discipline.

Shervani-Tabar, N. (M.S., Mechanical Engineering)

Stabilized Conservative Level Set Method with Adaptive Wavelet-based Mesh Refinement

Thesis directed by Prof. Oleg V. Vasilyev

This study investigates one of the well-known shortcomings of the conservative level set method, namely the ill-defined normal vector. A stabilized formulation is proposed which does not rely on the unit normal vector anymore. Instead, the proposed stabilized conservative level set, SCLS, utilizes a modified normal vector, magnitude of which is unit in the interfacial region of width ϵ and approaches zero in the far field from the interface. Respective adjustments have been applied on the reinitialization equation to comply with the proposed normal vector. This methodology is general and robust and it is not topology dependent. Since the information in the interfacial region are of a higher interest in comparison to the far field data, SCLS is specially well suited to be used with adaptive mesh refinement, AMR. In this research a general AMR-type approach named Adaptive Wavelet Collocation Method has been utilized, which makes use of wavelets to adapt on meshes in the interfacial region. A number of benchmark numerical problems have been performed to investigate the performance of the stabilized conservative level set approach. SCLS methodology is intended to be a base for simulation of interfacial phenomena, especially multiphase flows.

Dedication

To whoever might find this work interesting.

Acknowledgements

The author would like to express sincere gratitude and appreciation to his advisor professor Oleg V. Vasilyev for his excellent guidance, supervision, and encouragement during the course of this work. He genuinely cares about his students and rendered the author to believe in himself once again.

The author is extremely grateful to his very own heroes and beloved ones, Hakimeh and Mohammad, who made this opportunity possible for him to adventure a new world.

Many thanks are due to author's lab mates at multiscale modeling and simulation laboratory, Eric Brown-Dymkoski, Scott Wieland, and Nurlybek Kasimov, for their valuable comments.

Finally, author would like to thank his friends Sam, Enrique, Charles, and Reza for making Boulder feel like home.

Contents

Tables

Table

Figures

Figure

Chapter 1

Introduction

1.1 Interfacial Phenomena

Interface is the common boundary separating two immiscible phases. These two can be in the form of two similar phases, like a water-oil system or two non-similar phases, like a water-air system. Interfacial phenomena is refered to the behavior of the flows at the limit between the two phases. Due to vast presence of these phenomena in such disciplines as mechanical engineering, geophysics, biology, oceanography, and material science, much effort has been made to grasp their physics and chemistry. Drops, bubbles, soap films, wetting phenomena, surfactants, marangoni flows, and contact line dynamics are examples of these phenomena.

Experimental studies of interfacial phenomena are usually hard to conduct due to the nature of the interface. Hydrodynamic simulation of problems involving multiphase flows or multi-fluids is an important discipline within computational fluid dynamics. These problems normally involve a moving or deforming interface, which dictates severe difficulties to the study. A number of numerical methods have been developed for capturing the interface evolution. The main challenges that face the performance of these methods are mass conservation and discontinuity of material properties. Based on the depiction of interface in each method, interface capturing methods can be catagorized into two classes of Eulerian and Lagrangian methods.

Lagrangian methods are referred to a group of methods which trace the interface using markers. Front traking, marker, and particle-in-cell methods belong to this class. In front tracking methods marker particles are explicitly introduced to represent the moving front. These connected

set of particles can be described as moving internal boundaries. In the vicinity of the interface fluid evolution is computed using irregular meshes. While these schemes are faster than other particle methods, they pose many complications in reconstruction of the interface. The main drawback associated with this class is the the growing distortion in the distribution of the markers.

Eulerian methods are a class of interface capturing methods that define the interface as a scalar function. Some well known examples of this class include volume-of-fluid, boundary integral, and level set methods. In the volume-of-fluid method, a volume fraction is assumed for each cell in the domain. This volume fraction is defined as the area fraction of each cell located inside of the bounded interface. After each iteration of the advection equation the volume fraction is updated for the cells crossed by the interface and the interface is subsequently reconstructed based on the new fraction. The boundary integral methods can be applied to the fluids, whose governing partial differential equation is piecewise homogenious and could be represented or approximated by a Green's function. This group of methods is mainly used for simulation of inviscid potential flows. In these flows the effect of viscosity is neglected. Lastly, level set method describes fluid field as iso-contours of a signed distance function, which is the closest distance from each point in the domain to the interface including a sign that indicates whether the point is inside or outside of the bounded interface. Interface location is updated by advection of this function. Level set method is described in more details in the following section.

1.2 Level set method

Level set is a mathematical method to investigate the evolution of curves and surfaces. Level set has a wide range of applications in image processing, computer graphics, and Computational Fluid Dynamics (CFD). In fluid mechanics, propagation of the boundaries and interfaces occur in nature in the form of ocean waves, burning flames, bubble dynamics, etc. This method was first developed by Sethian in 1982 [25]. Given a continuous function $f(\mathbf{x})$, signed distance function $\phi(\mathbf{x}, t)$ represents the distance $d(\mathbf{x})$ between each point in the domain to the bounded zero level set of the function $f(\mathbf{x})$, i.e. $\mathbf{f} = 0$, with a sign indicating whether the point is inside or outside of the

bounded region. For simplicity, $\phi(\mathbf{x}, t)$ may be represented as $\phi(\mathbf{x})$ here. The zero level set is the zero iso-contour of $\phi(\mathbf{x})$ and represents an interface Γ in the domain R^d such that

$$\Gamma = \{\mathbf{x} \in R^d : f(\mathbf{x}) = 0\} \tag{1.1}$$

which bounds a region Ω of the domain R^d in a fashion that

$$\phi(\mathbf{x}, t) > 0 \qquad \text{if} \quad \mathbf{x} \in \Omega, \tag{1.2}$$

and

$$\phi(\mathbf{x}, t) \leq 0 \qquad \text{if} \quad \mathbf{x} \notin \Omega. \tag{1.3}$$

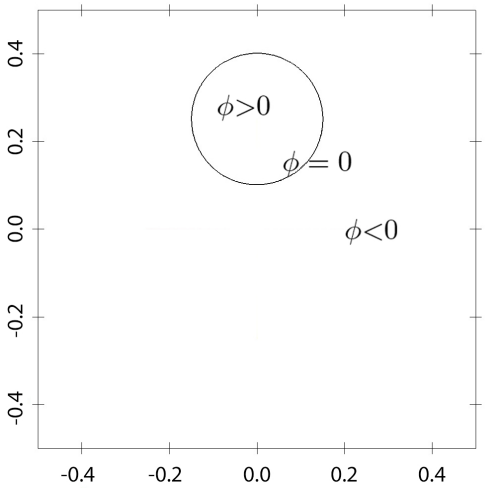

Figure 1.1: Schematic representation of signed distance function.

The main difference between level set method and other interface capturing methods is that in level set the front is defined by the zero iso-contour of a signed distance function $\phi(\mathbf{x})$ rather than set of points being evolved and interpolated to find the front. The main evolution equation of the level set method is [26]

$$\frac{\partial \phi}{\partial t} + (\mathbf{F} \cdot \nabla)\phi = 0 \tag{1.4}$$

where $\mathbf{F}$ denotes the speed of the front in the normal direction to the interface. This equation can also be reorganize in the form

$$\frac{\partial \phi}{\partial t} + \mathbf{u} \cdot \nabla \phi = 0 \tag{1.5}$$

where $\mathbf{u}$ expresses the velocity field in which the interface is being evolved. A unit normal vector $\mathbf{n}$ is defined as the unit vector in the normal direction with respect to the interface Γ. The direction of unit normal vector $\mathbf{n}$ is the same as gradient of signed distance function ϕ's [26]. Therefore, unit normal vector can be defined in terms of signed distance function ϕ as

$$\mathbf{n} = \frac{\nabla(\phi)}{|\nabla(\phi)|} \tag{1.6}$$

The distance function condition states that $|\nabla\phi(\mathbf{x})|$ be equal to unit at all time. At the beginning of the iterations, ϕ might be a signed distance function but later on, after ϕ has been evolved for some iterations, the function $f(\mathbf{x})$ may be distorted and the gradient gets out of hand. This especially happens when the velocity field $\mathbf{u}$ is not uniform. In this case, reinitialization is necessary to make the modulus of the gradient of the signed distance function $\phi(\mathbf{x})$ to be unit again. This ensures that for each unit step in the normal direction with respect to the interface Γ the value of distance function $d(\mathbf{x})$ also changes by 1. Therefore, a reinitialization procedure may be introduced to be applied on the signed distance function ϕ by solving the following Hamilton-Jacobi equation to steady state

$$\phi_\tau = \mathrm{sgn}(\phi^0)(1 - |\nabla\phi|) \tag{1.7}$$

with the initial condition

$$\phi^0 = \phi(\mathbf{x}, \tau), \tau = 0, \tag{1.8}$$

and the sign function $\mathrm{sgn}(\phi)$ defined as

$$\mathrm{sgn}(\phi) = \begin{cases} 1 & \text{if} \quad \phi{>}0, \\ 0 & \text{if} \quad \phi = 0, \\ -1 & \text{if} \quad \phi{<}0. \end{cases} \tag{1.9}$$

Note that τ indicates the pseudo time steps. This updated function has the same zero level set as the function $f(\mathbf{x})$ and provides with an updated value for signed distance function $\phi(\mathbf{x})$ that has the property of unity of the modulus of gradient of the signed distance function ϕ, or mathematically speaking $|\nabla\phi| = 1$.

The accuracy of the function $f(\mathbf{x})$ plays an important role when dealing with the level set method. Since step functions like sign function $\text{sgn}(\phi)$ have sudden changes, it is numerically hard to deal with them due to the possibility of introducing noise and oscilations to the solution. Therefore, a smoothed version of the sign function $\text{sgn}(\phi)$ based on Heaviside function $H(\phi)$ is used to compute the sign function in order to avoid instability. To smooth the edges, the Heaviside function is discretized as

$$H(\phi) = \begin{cases} 1 & \text{if} \quad \phi > \Delta\text{x}, \\ 0 & \text{if} \quad \phi < -\Delta\text{x}, \\ 0.5\left(1 + \frac{\phi}{\Delta x} + \frac{1}{\pi}\sin\left(\frac{\pi\phi}{\Delta x}\right)\right) & \text{Else.} \end{cases} \tag{1.10}$$

Then the sign function $\text{sgn}(\phi)$ is calculated based on the Heaviside function $H(\phi)$ as

$$\text{sgn}(\phi) = 2(\text{H}(\phi) - \frac{1}{2}). \tag{1.11}$$

Using explicit Euler method, reinitialization procedure could be discritized and expressed as following

$$\phi_i^{n+1} = \phi_i^n + \Delta\tau \cdot c \cdot \text{sgn}(\phi^0)|\nabla\phi^{\text{n}}| \tag{1.12}$$

where c is the constant added to the equation to meet the CFL condition. A first order upwind scheme could be implemented to discretize gradient of $\phi(\mathbf{x})$ in the equation above.

$$|\nabla\phi| = \begin{cases} \max(\max(D_x^-\phi_i, 0), \min(D_x^+\phi_i, 0)), \\ \\ \max(\min(D_x^-\phi_i, 0), \max(D_x^+\phi_i, 0)), \end{cases} \tag{1.13}$$

where

$$D_x^-\phi_i = \frac{\phi_i - \phi_{i-1}}{\Delta x} \tag{1.14}$$

and

$$D_x^+\phi_i = \frac{\phi_{i+1} - \phi_i}{\Delta x} \tag{1.15}$$

However, the conventional reinitialization method perturbs the front from its original location which subsequently results in a failure in conserving the area of the bounded region. In order to

overcome this difficulty, various methods have been proposed to improve the results of reinitialization procedure and enhance the volume conservation, the most influentials of which are proposed by Sussman and Fatemi [32], Russo and Smereka [23], and Enright et.al. [10].

Sussman and Fatemi in their novel work [32] suggested to put a constraint after solving the reinitialization Hamilton-Jacobi equation to prevent the straying of the zero level set from it's initial position at $\tau = 0$ due to the numerical errors of the reinitialization equation 1.7. Russo and Smereka [23] pointed out that when discretizing using equations 1.13 through 1.15, derivatives are calculated using upwind differencing according to the direction of the characteristics. Therefore, when differencing across the interface, this property will be violated and discretization of the derivatives in that region would not be truly upwind, because part of the information is coming from the wrong side of the level set. Hence, they offered a modification to the discretization of the gradient of the signed distance function within one cell from the front using the information that the signed distance function ϕ is zero on the interface Γ. Enright et.al. [10] proposed a hybrid particle tracing method to overcome the difficulty associated with the accuracy of the level set method. In their work, marker particles are distributed close to the interface on both sides of the zero level set. Detecting a particle in one side with initial location on the other side implies errors associated with the volume conservation of the level set method. Properties of the escaped particles are used to reconstruct the level set function. However, in this method redistribution of the makers is necessary after a while. Also, depending on the topology of the problem, special modifications might be required.

Qin et.al [21], on the other hand, have came up with a different methodology. They suggested that reconstruction of the signed distance function by geometrically projecting interface topology onto Cartesian grid using a second-order accurate interpolation can help with preventing the reinitialization errors to amplify. In this method not only is the reinitialization step kept, but also the results are modified after each iteration by reconstruction of the signed distance function ϕ.

Although the proposed methods alleviate the error accumulation, the main shortcoming of the conventional level set method is still its non-conservative nature. Therefore, it might violate

the physics of the problem by gaining or losing mass, which can lead to serious errors. This has resulted in attempts to come up with a new level set method formulation which conserves the area within the interface.

Olsson and Kreiss [19] in their novel work proposed a new conservative level set method. In this method, the two fluids in problem are represented by level set equal to 1 or 0, respectively. This helps to emphasis the discontinuous nature of the interface. For the sake of numerical robustness, interface is considered in a transitional region with thickness ϵ within the limit of two fluids. Level set goes smoothly from 0 to 1 in this zone and the interface itself would be recognized as 0.5 level. In other words

$$\Gamma = \{\mathbf{x} \in R^d : f(\mathbf{x}) = 0.5\} \tag{1.16}$$

Sharper change in this zone would result in a lower conservation error. This requires a choice of thinner interfacial region thickness ϵ. However, very low ϵ may cause numerical difficulties. Therefore, choosing the most suitable value of ϵ is a matter of balance between a low conservation error and a reasonable resolution [8].

When the conservative level set method is employed fluids and the interface are no more defined as the signed distance function $\phi(\mathbf{x})$. In the conservative level set method, instead, level set is defined as a regularized characteristic function

$$\psi(\mathbf{x}) = \frac{1}{1 + e^{-\frac{\phi(\mathbf{x})}{\epsilon}}} \tag{1.17}$$

which could be reformulated as a modified hyperbolic tangent function

$$\psi(\mathbf{x}) = 0.5(tanh((2\epsilon)^{-1}\phi(\mathbf{x})) + 1) \tag{1.18}$$

Advection of the signed distance function ϕ in conventional level set method has not been done in a conservative way. In the conservative level set method a conservative version of equation 1.5 can be rewritten as

$$\frac{\partial \psi}{\partial t} + \nabla \cdot (\psi \mathbf{u}) = 0 \tag{1.19}$$

Furthermore, an intermediate step should be added to this equation to preserve the shape and the thickness of the interface zone. In order to do so, an artificial compression term is added in the form of a hyperbolic differential equation

$$\frac{\partial \psi}{\partial \tau} + \nabla \mathbf{f}(\psi) = 0 \tag{1.20}$$

Where $\mathbf{f}$ represents the compressive function. This function should be applied in the region where $0<\psi<1$ and in the direction of normal vector $\mathbf{n}$. Hence, the function for the compressive term $\mathbf{f}$ can be defined in terms of the mathematical expression

$$\mathbf{f} = \psi(1-\psi)\mathbf{n} \tag{1.21}$$

A small viscosity is added in order to avert discontinuities at surface. Therefore

$$\frac{\partial \psi}{\partial \tau} + \nabla \mathbf{f}(\psi) = \epsilon \Delta \psi \tag{1.22}$$

where ϵ regulates the amount of diffusive term and hence the thickness of the interface transitional zone. Eventually, the conservative level set method consists of a conservative advection and a corresponding reinitialization procedure

$$\frac{\partial \psi}{\partial \tau} + \nabla \cdot (\psi(1-\psi)\mathbf{n}) = \epsilon \Delta \psi \tag{1.23}$$

to recover the shape.

However, the viscosity introduced in equation 1.22 applies to the interface in every direction. Whereas, the compression term only acts in the normal direction to the surface, which renders the final result unbalanced. In other words, the compression term balances the normal diffusion. But the tangential diffusion remains unbalanced and therefore it might move or distort the interface. In order to overcome this difficulty, Ollson et. al. further developed their proposed method [20]. They introduced a refinement on the diffusive term to apply it just in the normal direction with respect to the interface Γ. The resulting equation is

$$\frac{\partial \psi}{\partial \tau} + \nabla \cdot (\psi(1-\psi)\mathbf{n}) = \nabla \cdot (\epsilon(\nabla \psi \cdot \mathbf{n})\mathbf{n}) \tag{1.24}$$

which offers a diffusive flux only normal to the surface.

In comparison with the conventional level set method, using a hyperbolic tangent initial condition has some flaws, one of which is the complications with finding normal. Traditionally, unit normal vector $\mathbf{n}$ is computed using the equation 1.6. In the conservative formulation a hyperbolic tangent $\psi(\mathbf{x})$ of the signed distance function $\phi(\mathbf{x})$ is being advected. Hence, the signed distance function $\phi(\mathbf{x})$ is no longer directly accessible. Olsson [19][20] used the $\psi(\mathbf{x})$ to calculate the normal by using

$$\mathbf{n} = \frac{\nabla(\psi)}{|\nabla(\psi)|} \tag{1.25}$$

This equation gives accurate results in the interfacial region. However, in the far field that ψ is either 0 or 1, the gradient of ψ becomes very small and results in drastical change of direction of unit normal vector $\mathbf{n}$ in far field. This makes the method less favorable to get employed to compute the normal. In an effort to fix this issue, one may use an inverse hyperbolic tangent to recycle the ϕ from ψ, namely using

$$\phi(\mathbf{x}) = \epsilon ln(\frac{\psi(\mathbf{x})}{1-\psi(\mathbf{x})}) \tag{1.26}$$

The problem with this formulation is that although it gives good results near the 0.5 iso-surface, the results far from the interface might not be dependable.

Desjardins et. al. [8] proposed a new method to reconstruct a smoothed signed distance function field $\phi(\mathbf{x})$ from hyperbolic tangent function $\psi(\mathbf{x})$ by combining the conservative level set method with a redistancing algorithm performed using Fast Marching Method, FMM.

Shukla et. al. [30] suggested to avoid calculating unit normal vector $\mathbf{n}$ directly from ψ by employing an auxiliary function γ which is essentially a smoother version of ψ and helps with a better estimation of the gradients. Figure 1.2 shows how the auxiliary function γ smooths the hyperbolic function ψ.

Zhao et. al. [40] recommended to use the inverse hyperbolic tangent in equation 1.26 to recycle the signed distance function ϕ in the regions close to the interface Γ and advect the conventional level set equation coupled with the conservative level set method to find the unit normal

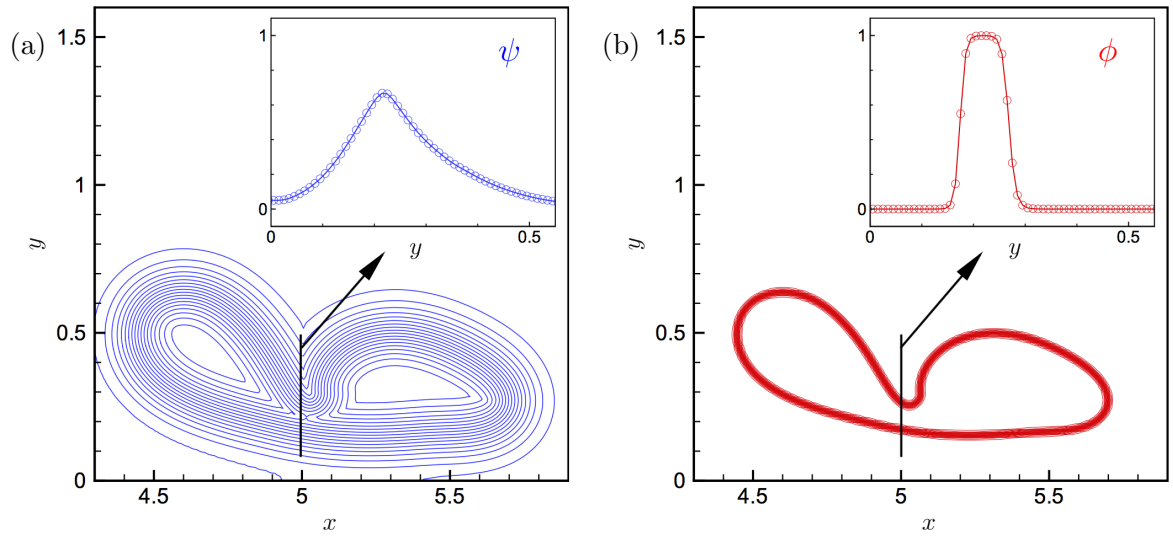

Figure 1.2: A comparison between the isolevels of (a) hyperbolic tangent function ψ and (b) auxiliary function γ [8].

vector directly by plugging in ϕ into equation 1.6 in the far field.

Conservative level set method is robust and general and does not require special treatments and can automatically be applied. Moreover, higher resolution is only needed in the vicinity of the interfacial region while the flow field can be accurately solved in the far field using a coarser resolution. These properties make Conservative Level Set a desirable method in context of the adaptive mesh refinement, AMR, methods. A wavelet-based AMR-type solver has been used in this study to carry out the numerical simulations.

1.3 Wavelets

Joseph Fourier introduced the idea of expansion or approximation of a periodic function $f(x)$ in terms of trigonometric series. These series, formally known as Fourier series, take advantage of the orthogonality relationship of the sine and cosine functions. First intended for the solution of the heat equation in a metal plate, Fourier series of $f(x)$ on interval $(-l, l)$ are defined as

$$f(x) = \sum_{n=-\infty}^{+\infty} c_n e^{\frac{in\pi x}{l}} \tag{1.27}$$

where

$$c_n = \frac{1}{2l} \int_{-l}^{+l} f(t) e^{-\frac{in\pi x}{l}} dt \tag{1.28}$$

Assuming $l \to \infty$ we have

$$f(x) = \frac{1}{2\pi} \int_{-\infty}^{+\infty} e^{i\omega x} d\omega \int_{-\infty}^{+\infty} e^{-i\omega t} f(t) dt \tag{1.29}$$

Fourier series solution of PDE's was considered a remarkable success in it's own time. However, it has two major drawbacks. Firstly, it is not intended to represent local information in time, meaning that they capture global behavior of a function. This is because the constitutive functions of Fourier series are not all localized in time. Secondly, although it provides the opportunity to investigate the problem either in spatial domain or frequency domain, it doesn't provide a chance to study both together [7]. To overcome these difficulties wavelets were introduced in 1980's. Hence, wavelets are referred to as a departure from Fourier analysis [14].

Wavelets, (although many believe that the idea roots back to the 30's [14]), introduced in 1984 by Grossmann and Marlet, have significantly affected the science and technology [13]. Mathematical modeling, signal processing, and speech recognition are among the earliest areas to be impacted by wavelets. The first utilization of the wavelets in fluid mechanics dates back to early 90's [11]. The unique properties of wavelets have introduced them as a suitable choice to solve the Partial Differential Equations (PDE's) on adaptive grids [24].

Wavelets are a class of basis functions that are localized in both physical space and wavenumber space. Because of these properties, wavelets, unlike the Fourier transform which provides frequency information only, provide both spatial and frequency information. Wavelet-based algorithms show a number of properties due to their controllable localization in both time and space [3].

Other wavelet properties include efficient multiscale decompositions, existence of recursive O(N) fast wavelet transform, and preconditioning and compression of operators and matrices. These properties have resulted in utilization of wavelets in developing of partial differential equation, PDE, solvers. Most kinds of linear PDEs have been solved using wavelet based methods. There also exist many adaptive wavelet methods developed to solve different nonlinear PDEs.

The wavelet based methods are generally classified into two categories of wavelet-Galerkin

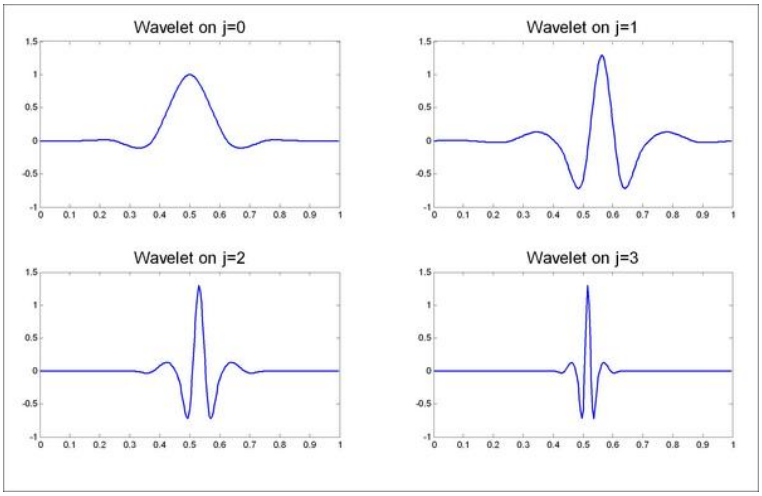

Figure 1.3: Sample wavelets on varying levels of resolution.

and wavelet-collocation. The former solves the problem in the coefficient space, while the latter solves it in the physical space. In the wavelet collocation method every wavelet coefficient is paired with a grid point in the computational domain to represent the flow variables. This property makes it simple to calculate the nonlinear terms.

Currently, two classes of wavelets have been introduced. The first class of wavelets ψ_i^j are defined as

$$\psi_i^j(\mathbf{x}) = 2^{0.5j}\psi(2^j x - k) \tag{1.30}$$

This family of functions is technically the translation and dilation of a mother wavelet, ψ, and they were primarily constructed using the Fourier transform [37]. These functions are defined recursively and are generated via an iterative algorithm [3].

A second class of wavelets was introduced by Sweldens in 1996. Wavelets of the second generation, which are a generalization of bi-orthogonal wavelets, are constructed in the physical space without the requirement of translation and dilation invariance. They are generally created using lifting scheme or interpolating wavelet transform [37].

Wavelet collocation method compresses functions with localized structures or regions with sharp transition very well using wavelet decomposition. Equation 1.31 expresses an arbitrary flow

variable, $u(\mathbf{x})$, in terms of wavelet basis functions:

$$u(\mathbf{x}) = \sum_{i \in I_\phi^0} \bar{u}_i^0 \phi_i^0(\mathbf{x}) + \sum_{j=0}^{+\infty} \sum_{\mu=1}^{2^d-1} \sum_{i \in I_\psi^{\mu,j}} \tilde{u}_i^{\mu,j} \psi_i^{\mu,j}(\mathbf{x}) \tag{1.31}$$

where $\bar{u}_i^0$ and $\tilde{u}_i^j$ represent scaling and wavelet coefficients and $\phi_i^0(\mathbf{x})$ and $\psi_i^j(\mathbf{x})$ express scaling functions on the coarsest level of resolution and wavelet basis functions of different levels of resolution j, respectively. Superscripts μ denote different families of wavelets and d stands for the dimension. The wavelet coefficients $\tilde{u}_i^j$ have small values except for the regions close to the large gradients.[22]

A thresholding criterion, ε, can be defined to divide the wavelet coefficients into two groups, which results in breakdown of $u(\mathbf{x})$ into two functions

$$u_{\geqslant}(\mathbf{x}) = \sum_{i \in I_\phi^0} \bar{u}_i^0 \phi_i^0(\mathbf{x}) + \sum_{j=0}^{+\infty} \sum_{\mu=1}^{2^d-1} \sum_{\substack{i \in I_\psi^{\mu,j} \\ |\tilde{u}_i^{\mu,j}| \geqslant \varepsilon \|u\|}} \tilde{u}_i^{\mu,j} \psi_i^{\mu,j}(\mathbf{x}) \tag{1.32}$$

and

$$u_{<}(\mathbf{x}) = \sum_{j=0}^{+\infty} \sum_{\mu=1}^{2^d-1} \sum_{\substack{i \in I_\psi^{\mu,j} \\ |\tilde{u}_i^{\mu,j}| < \varepsilon \|u\|}} \tilde{u}_i^{\mu,j} \psi_i^{\mu,j}(\mathbf{x}) \tag{1.33}$$

such that

$$u(\mathbf{x}) = u_{\geqslant}(\mathbf{x}) + u_{<}(\mathbf{x}) \tag{1.34}$$

As a result of this split, compression can be achieved by keeping only the wavelets with the coefficients greater than ε. In other words, high resolution computation is only performed where it is necessary and a significant reduction in number of required points can be achieved; while the accuracy is kept at the desired level. This results in an optimized use of computational resources by approximation of the solution with an error of $O(\varepsilon)$.

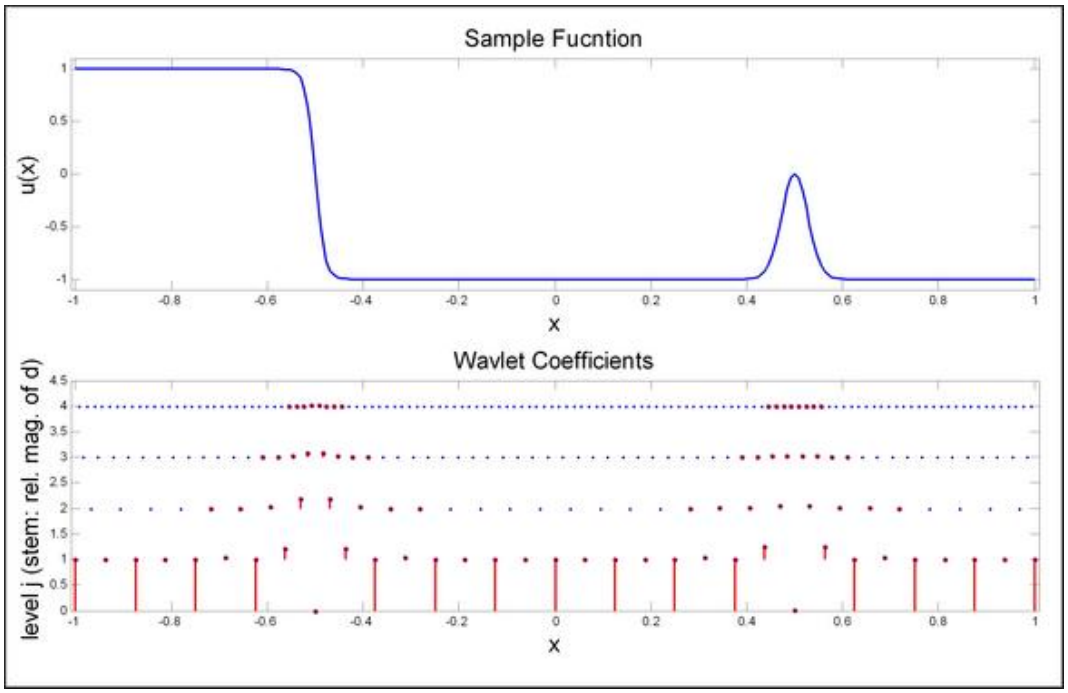

Figure 1.4: Wavelet decomposition of a sample function. The red points are the points necessary to accurately represent the function.

1.4 Adaptive Wavelet-collocation Method

The numerical examples in this research may involve localized structures or sharp transitions. These problems necessitate high resolution computation in the transition area, as the transition may fall between the grids. Hence, using a uniform grid would be impractical.

In this study, a general numerical technique for solving linear and nonlinear partial differential equations named Adoptive Wavelet Collocation Method AWCM has been engaged with a Stabilized Conservative Level Set, SCLS, to develop a methodology for tracking the front of a bounded interface. In the rest of this section the methodology used in AWCM would be reviewed. Interested reader is refered to reference [24] for detailed discussion on AWCM and it's parallel implementation.

Adaptive solution of nonlinear partial differential equations is performed by adaptive wavelet collocation method based on bi-orthogonal lifted interpolating wavelets to construct a computational grid adapted to the solution. The wavelet decomposition naturally provides a set of nested multi-scale grids adapted to the solution, and we take advantage of this property in the solver. The method presented here uses the multi-scale wavelet decomposition as the basis for an adaptive multilevel method for nonlinear elliptic equations.

A wavelet decomposition is used in AWCM to dynamically adopt on steep gradients in the solution during evolution of the flow by spliting the flow field $u(\mathbf{x})$ into two groups with coefficients larger or smaller than the product of a non-dimensional thresholding parameter, ε, and the dimensional scale $\|u\|$.

AWCM uses wavelet properties to determine, on the fly, significant points needed for an accurate solution [24]. To include the points which can potentially become significant in the next time step, the adjacent points to the significant wavelet coefficients are also included in the computational grid. This way, the grid would be able to automatically follow the evolution of the solution.

Then, reconstruction points are added to compute the wavelet transforms. Finally, ghost points are introduced to compute spatial derivatives. It is noteworthy that the spatial derivatives

are calculated using the finite difference methods. Addition of the ghost points helps to maintain the desired order of the method. [18]

Despite their short existence, many wavelet techniques have been developed for numerical simulations of compressible and incompressible Euler and Navier-Stokes equations for both inert and reactive flows. The ability to precisely identify, isolate, and track localized, dynamically dominant flow structures such as shocks and flame fronts on adaptive computational meshes has distinguished wavelet techniques from conventional methods [24].

Wavelet techniques in CFD are a relatively new and advancing area, which involve many challenging issues to be investigated.

Chapter 2

Stabilized Conservative Level Set Method with Adaptive Wavelet-based Mesh Refinement

This chapter includes a submitted paper, which contains the numerical results and computational examples.

2.1 Introduction

Interfacial phenomena are quite common in fluid mechanics, e.g. bubbles and drops, waves, and liquid films [28, 2, 12, 15]. Surface or interface tracking methods can be roughly divided into two classes: 1) interface tracking methods where the interfaces are represented explicitly, [**?**, e.g.,]]univerdi-tryggvason:1992,rider-kothe:1998 and 2) level set methods, where the interfaces are represented implicitly by an isosurface or level set of a function [**?**, e.g.,]]sethian1999level,osher-fedkiw:2003. The main advantage of level set methods compared to the interface tracking approaches is that the former handle topological changes such as merging and breaking more easily.

Level set approach was originally developed by Sethian [25]. Given a continuous level set function $f(\mathbf{x}, t)$, the interface $\Gamma(t)$ is defined as

$$\Gamma(t) = \{\mathbf{x} \in R^d : f(\mathbf{x}, t) = 0\}, \tag{2.1}$$

which bounds a region $\Omega(t)$ of the domain R^d. The signed distance level set function $\phi(\mathbf{x}, t)$ is defined as

$$\phi(\mathbf{x}, t) = \mathcal{I}(\mathbf{x}, t) \min_{\mathbf{y} \in \Gamma(t)} \|\mathbf{x} - \mathbf{y}\|_2 \ , \tag{2.2}$$

where $\mathcal{I}(\mathbf{x}, t)$ is a sign function that indicates, whether $\mathbf{x}$ is inside or outside of the region Ω

$$\mathcal{I}(\mathbf{x}, t) = \begin{cases} 1, & \text{if } \mathbf{x} \in \Omega(t) \\ -1, & \text{if } \mathbf{x} \notin \Omega(t) \end{cases}, \tag{2.3}$$

while the zero level set defines the interface $\Gamma(t)$ itself.

The evolution equation of the level set function $\phi(\mathbf{x}, t)$ is given by

$$\frac{\partial \phi}{\partial t} + \mathbf{u} \cdot \nabla \phi = 0, \tag{2.4}$$

where $\mathbf{u}$ is the velocity field. The unit normal vector can be computed as

$$\mathbf{n} = \frac{\nabla \phi}{|\nabla \phi|}, \tag{2.5}$$

where for the level set function $\phi(\mathbf{x}, t)$ the distance function condition

$$|\nabla \phi(\mathbf{x}, t)| = 1 \tag{2.6}$$

should be satisfied. Note that the evolution of $\phi(\mathbf{x}, t)$ according to (2.4) does not automatically guarantee the satisfaction of condition (2.6). As a result, the level set function can be distorted and no longer represent true distance function, thus, necessitating introduction of a reinitialization procedure to reinforce condition (2.6). For reinitialization procedure Sussman et al. [33] proposed to solve the following Hamilton-Jacobi equation to steady state

$$\frac{\partial \tilde{\phi}}{\partial \tau} + \operatorname{sgn}(\phi)(|\nabla \tilde{\phi}| - 1) = 0, \tag{2.7}$$

$$\tilde{\phi}(\mathbf{x}, 0) = \phi(\mathbf{x}, t), \tag{2.8}$$

where τ is the pseudo time, $\operatorname{sgn}(x) = 2H(x) - 1$ is the signum function, and $H(x)$ is the Heaviside function. In practice the Eq. (2.7) needs to be solved for $\tau = O(\epsilon)$ to guarantee condition (2.6) in the band of width ϵ around interface $\Gamma(t)$. In fact, depending on the computational approach, the level set function may be defined only in the narrow band, if the information far from the interface is not used by the algorithm.

One of the main difficulties of the level set approach, especially in the context of incompressible flows, is the volume conservation, since traditional level set methods, even rewritten in

divergence form for the divergence-free velocity field, do not guarantee the volume preservation. In order to overcome this difficulty, different methods have been proposed to improve the results of reinitialization procedure and enhance the volume conservation, the most influential of which are proposed by Sussman and Fatemi [32], Russo and Smereka [23], and Enright et.al. [10]. Sussman and Fatemi suggested to add an additional constraint after solving the reinitialization Hamilton-Jacobi equation [32]. Russo and Smereka offered a modification to the discretization of the gradient of the signed distance function within one cell from the front using the information that ϕ is zero on the interface [23]. Enright et.al. [10] have proposed a particle tracing method to overcome the difficulty associated with the accuracy of the level set method, where marker particles are used to reconstruct the level set function.

In an attempt to construct a level set approach with built-in volume preserving properties Olsson and Kreiss [19] proposed a conservative level set method utilizing a regularized level set function

$$\psi(\mathbf{x},t) = \frac{1}{1+e^{-\frac{\phi(\mathbf{x},t)}{\epsilon}}} = \frac{1}{2}\left(\tanh\left(\frac{\phi(\mathbf{x})}{2\epsilon}\right)+1\right), \tag{2.9}$$

which changes between 0 and 1 in the narrow region with thickness $O(\epsilon)$. The interface Γ is represented by

$$\Gamma(t) = \{\mathbf{x} \in R^d : \psi(\mathbf{x},t) = 0.5\}. \tag{2.10}$$

Being formulated for incompressible flows, the evolution of $\psi(\mathbf{x},t)$ is governed by the advection equation written in conservative form

$$\frac{\partial \psi}{\partial t} + \nabla \cdot (\psi \mathbf{u}) = 0. \tag{2.11}$$

In the limit of interface thickness ϵ going to zero the integral $\int_{\Omega(t)} \psi(\mathbf{x},t)d\mathbf{x}$ approaches the volume of the region $\Omega(t)$, defined by $\int_{\Omega(t)} d\mathbf{x}$

$$\int_{\Omega(t)} \psi(\mathbf{x},t)d\mathbf{x} = \int_{\Omega(t)} d\mathbf{x} + O(\epsilon). \tag{2.12}$$

Furthermore, it was shown in Ref. [20] that for smooth interface boundaries

$$\int_{\Omega(t)} d\mathbf{x} = \int_{\Omega(0)} d\mathbf{x} + O(S_\Gamma \kappa_\Gamma \epsilon^2), \tag{2.13}$$

where S_Γ and κ_Γ are respectively interface surface area (length) and maximum curvature. Thus, in contrast to the conventional level set approaches, the conservative level set method maintains rigorous control of the volume conservation error through *a priori* chosen interface thickness parameter ϵ.

Similarly to the conventional level set approaches, one needs to add a reinitialization procedure to guarantee that the structure and thickness of the interface zone given by Eq. (2.9) is preserved. For the renormalization procedure Olsson and Kreiss [19] proposed to solve the following reinitialization equation

$$\frac{\partial \psi}{\partial \tau} + \nabla \cdot (\psi(1-\psi)\mathbf{n}) = \nabla \cdot (\epsilon \nabla \psi), \tag{2.14}$$

where term $\psi(1-\psi)\mathbf{n}$ is the compressive flux term, forcing the level set function $\psi(\mathbf{x}, \tau)$ towards the interface $\Gamma(t)$ in the normal direction, and the term on the right hand side of Eq. (2.14) the diffusion term, which controls the thickness of the interface region. The unit normal vector $\mathbf{n}$ is computed from (2.5) using relation (2.9) resulting in

$$\mathbf{n} = \frac{\nabla(\psi)}{|\nabla(\psi)|}. \tag{2.15}$$

Realizing that the homogeneous diffusion term in reinitialization procedure (2.14) results in unbalanced tangential diffusion, which could move the interface, Ollson et al. [20] proposed further improvement of the conservative level set method by limiting the diffusion term to only normal direction with respect to the interface. The resulting equation becomes

$$\frac{\partial \psi}{\partial \tau} = -\nabla \cdot (\psi(1-\psi)\mathbf{n}) + \nabla \cdot (\epsilon(\nabla \psi \cdot \mathbf{n})\mathbf{n}). \tag{2.16}$$

In comparison with the conventional level set approaches, the conservative level set method has one major difficulty, namely, ill-conditioned behavior of the normal vector, defined by Eq. (2.15). In traditional level set approaches, the normal vector $\mathbf{n}$ is computed using the equation (2.5), with $|\nabla \phi|$ being unity or close to unity. In the conservative level set formulation, a hyperbolic tangent of the signed distance function is being advected. Hence, the signed distance function is no longer

directly accessible. Olsson et al. [19, 20] used the $\psi(\mathbf{x}, t)$ to calculate the normal. However, this way the normal is highly sensitive to the changes in $\psi(\mathbf{x})$ far from interface, resulting in noisy normal vector field in the regions where $|\psi|$ approaches constant value. This makes the method less favorable to get employed to compute the normal. A number of approaches to stabilize the calculation of normal vector has been proposed. One way is to utilize an inverse hyperbolic tangent to recycle the ϕ from ψ

$$\phi(\mathbf{x}) = \epsilon \ln(\frac{\psi(\mathbf{x})}{1 - \psi(\mathbf{x})}). \tag{2.17}$$

Zhao et al. [40] state that although this method somewhat improves the ill-conditioning behavior of Eq. (2.15), it still results in a noisy normal vector far from interface boundary, mainly because the numerical error is still dominant there. They proposed to use the inverse hyperbolic tangent in equation (2.17) to recycle ϕ in the regions close to the interface and in addition, to advect the conventional level set equation so that the definition (2.5) can be used to find the normal in the regions far from Γ. Shukla et al. [30] suggested to use an auxiliary function $\gamma(\psi)$ to calculate the normal, where the function is defined as

$$\gamma = \frac{\psi^{\alpha}}{\psi^{\alpha} + (1 - \psi)^{\alpha}}, \tag{2.18}$$

for the parameter $\alpha < 1$, which measures the ratio of interface thickness of ψ and γ. Desjardins et al. [8] proposed a method to recycle ϕ. They implemented Fast Marching Method (FMM) to reconstruct the signed distance function, ϕ, from the hyperbolic tangent function, ψ. Although this approach was better conditioned than the above mentioned methods, it lacks generality and required additional computational efforts.

In this paper we propose novel stabilized conservative level set approach that addresses the main shortcoming of the conservative level set method. An alternative reinitialization procedure is proposed, which no longer requires the normal vector far from the interface boundary. The proposed approach is robust and general. Due to completely analytical formulation, the proposed methodology is ideal for use in combination with adaptive mesh refinement (AMR) methods (see e.g., Aftosmis, Berger and Melton, Chapter 22 in Ref. [35]). The use of AMR allows adequate

resolution of the moving and deformable interface regions without over-resolving solution fields away from the interface. All of the results reported in this paper are obtained using the Adaptive Wavelet Collocation Method (AWCM) [37, 38, 36, 18], which utilizes a wavelet decomposition to dynamically adapt on localized structures of the solution while retaining a predetermined order of accuracy.

2.2 Stabilized Conservative Level Set method

The ill-conditioned behavior of the normal vector $\mathbf{n}$ away from the interface not only affects the accuracy of the evolution of the level set defined by Eq. (2.16), but also could lead to the numerical instabilities. In this paper, an alternative formulation, which no longer relies on the unit normal vector $\mathbf{n}$, is presented. The proposed Stabilized Conservative Level Set makes use of an alternative normal vector with diminishing magnitude away from the interface defined as:

$$\mathbf{m} = \frac{\epsilon \nabla \psi}{\left(\epsilon^2 \left|\nabla \psi\right|^2 + \alpha^2 \exp\left(-\beta \epsilon^2 \left|\nabla \psi\right|^2\right)\right)^{1/2}}, \tag{2.19}$$

where ϵ is the interface thickness parameter, while α and β are constants defining the region where vector $\mathbf{m}$ is approximately a unit vector. In practical applications, the interface thickness parameter, ϵ, is defined in terms of local mesh resolution, Δx:

$$\epsilon = \delta \Delta x. \tag{2.20}$$

In the vicinity of the interface, the term $\epsilon|\nabla\psi|$ is approaching unity, which for appropriately chosen parameters α and β results in a negligible second term in the denominator, ultimately resulting in $\mathbf{m}$ approaching $\mathbf{n}$. However, in the regions far from the interface, the magnitude of the vector $\mathbf{m}$ goes to zero. This property of the non-normalized vector $\mathbf{m}$ makes it possible to introduce an alternative reinitialization equation by realizing that in the Eq. (2.16) the diffusion in the interface normal direction is only important in the immediate vicinity of the interface, while in the regions away from the interface the homogeneous diffusion as in Eq. (2.14) is more appealing. Replacing the unit normal vector $\mathbf{n}$ by the new vector $\mathbf{m}$ and adding an additional diffusion term that ensures the

right asymptotic behavior close to and away from the interface, results in the following alternative reinitialization equation:

$$\frac{\partial \psi}{\partial \tau} = -\nabla \cdot (\psi(1-\psi)\mathbf{m}) + \nabla \cdot (\epsilon(\nabla\psi \cdot \mathbf{m})\mathbf{m}) + \nabla \cdot ((1-|\mathbf{m}^2|)\epsilon\nabla\psi). \tag{2.21}$$

Note that if a unit normal vector $\mathbf{n}$ is used instead of $\mathbf{m}$, the Eq. (2.21) automatically reduces to Eq. (2.16). In practical implementation, while the reinitialization procedure may consist of several pseudo iterations, the $\mathbf{m}$ vector needs to be updated only once at the beginning of the pseudo iterations.

2.3 Numerical Implementation

When modeling evolution of the level set using Eq. (2.21) it is essential that the interface thickness is substantially smaller than the curvature of the interface, which, in turn, necessitates high resolution in the areas close to the interface. On the other hand, in the regions far from the interface the resolution requirements may be substantially lower. Adaptive mesh refinement methods are ideally suited for use with Stabilized Conservative Level Set (SCLS) approach. In this study, a general AMR-type numerical method for solving partial differential equations based on bi-orthogonal lifted interpolating wavelets [34] has been used to demonstrate the ability of the SCLS methodology to accurately track the interface. For the reader's convenience the Adaptive Wavelet Collocation Method (AWCM) is briefly reviewed next. For the detailed description of the method and its parallel implementation the reader is referred to Refs. [38, 36, 18].

Wavelets are a class of oscillatory basis functions of finite duration. Unlike sines and cosines that have global support, wavelets are localized in both physical and wave-number space. The need to have both position and frequency information was one of the main motivations that led to the development of wavelets as an alternative to the Fourier transform [31]. A multi-resolution wavelet representation of a field $u(\mathbf{x})$ can be formally written as

$$u(\mathbf{x}) = \sum_{\mathbf{k}\in\mathbf{I}_\phi^0} \bar{u}_{\mathbf{k}}^0 \phi_{\mathbf{k}}^0(\mathbf{x}) + \sum_{j=0}^{+\infty} \sum_{\mu=1}^{2^d-1} \sum_{\mathbf{k}\in\mathbf{I}_\psi^{\mu,j}} \tilde{u}_{\mathbf{k}}^{\mu,j} \psi_{\mathbf{k}}^{\mu,j}(\mathbf{x}), \tag{2.22}$$

where $\bar{u}^0_{\mathbf{k}}$ and $\tilde{u}^{\mu,j}_{\mathbf{k}}$ represent scaling and wavelet coefficients, while $\phi^0_{\mathbf{k}}(\mathbf{x})$ and $\psi^{\mu,j}_{\mathbf{k}}(\mathbf{x})$ express scaling functions at the coarsest level of resolution and wavelet basis functions of different levels of resolution, j, respectively. Superscript μ denotes the different families of wavelets and d stands for the dimension. Multi-resolution decomposition (2.22) provides a natural platform to construct adaptive numerical methods based on the analysis of the wavelet coefficients, $\tilde{u}^{\mu,j}_{\mathbf{k}}$, which, in general, have small values except for the regions close to the large gradients [22]. Formally, the field $u(\mathbf{x})$ can be decomposed into two sub-fields

$$u(\mathbf{x}) = u_{\geqslant}(\mathbf{x}) + u_{<}(\mathbf{x}) \tag{2.23}$$

defined by

$$u_{\geqslant}(\mathbf{x}) = \sum_{\mathbf{k}\in\mathbf{I}^0_\phi} \bar{u}^0_{\mathbf{k}}\phi^0_{\mathbf{k}}(\mathbf{x}) + \sum_{j=0}^{+\infty}\sum_{\mu=1}^{2^d-1} \sum_{\substack{\mathbf{k}\in\mathbf{I}^{\mu,j}_\psi \\ |\tilde{u}^{\mu,j}_{\mathbf{k}}|\geqslant\varepsilon\|u\|}} \tilde{u}^{\mu,j}_{\mathbf{k}}\psi^{\mu,j}_{\mathbf{k}}(\mathbf{x}) \tag{2.24}$$

and

$$u_{<}(\mathbf{x}) = \sum_{j=0}^{+\infty}\sum_{\mu=1}^{2^d-1} \sum_{\substack{\mathbf{k}\in\mathbf{I}^{\mu,j}_\psi \\ |\tilde{u}^{\mu,j}_{\mathbf{k}}|<\varepsilon\|u\|}} \tilde{u}^{\mu,j}_{\mathbf{k}}\psi^{\mu,j}_{\mathbf{k}}(\mathbf{x}), \tag{2.25}$$

where $\varepsilon > 0$ is the non-dimensional (relative) thresholding parameter defining the decomposition and $\|u\|$ is the (absolute) dimensional scale. As a result of this split, the compression can be achieved by keeping only the wavelets with coefficients greater than $\varepsilon\|u\|$. In other words, high resolution computation is only performed where it is necessary and a significant reduction in the number of required wavelets can be achieved. The AWCM takes advantage of the wavelet compression properties (2.24) and one-to-one correspondence between wavelets and the corresponding grid points on a multi-level computational mesh. As a result the AWCM has the ability to identify, isolate, and track localized, dynamically dominant flow structures, such as interfaces, on adaptive computational mesh while **a priori** controlling the accuracy of the solution at the desired level $O(\varepsilon)$. This property has distinguished wavelet techniques from conventional methods [24].

2.4 Numerical Results and Discussion

Three numerical benchmark tests have been performed to investigate the performance of the proposed Stabilized Conservative Level Set method. The interface in each example is defined as the $\psi(\mathbf{x}) = 0.5$ level set of a hyperbolic tangent function defined by Eq. (2.9). Krylov time integration method [9] with 6-th order wavelet approximation is used to solve the evolution equation (2.11) in all benchmark tests. The reinitialization equation (2.21) is integrated for each convective time step. For all test problems in this section an explicit Euler integration with $CFL_\tau = 0.01$ and 5 pseudo iterations per convective time step has been used to perform the reinitialization procedure. All numerical results are obtained with $\alpha = 10^{-4}$ and $\beta = 10$ corresponding to the interface thickness of order $O(6\epsilon)$, which was found to be optimal: sufficiently large interface zone with $\mathbf{m}$ approaching unit normal vector and small enough to minimize the computational cost, which increases with the growth of the interface thickness. For all numerical simulations the effective grid resolution in all directions was kept the same.

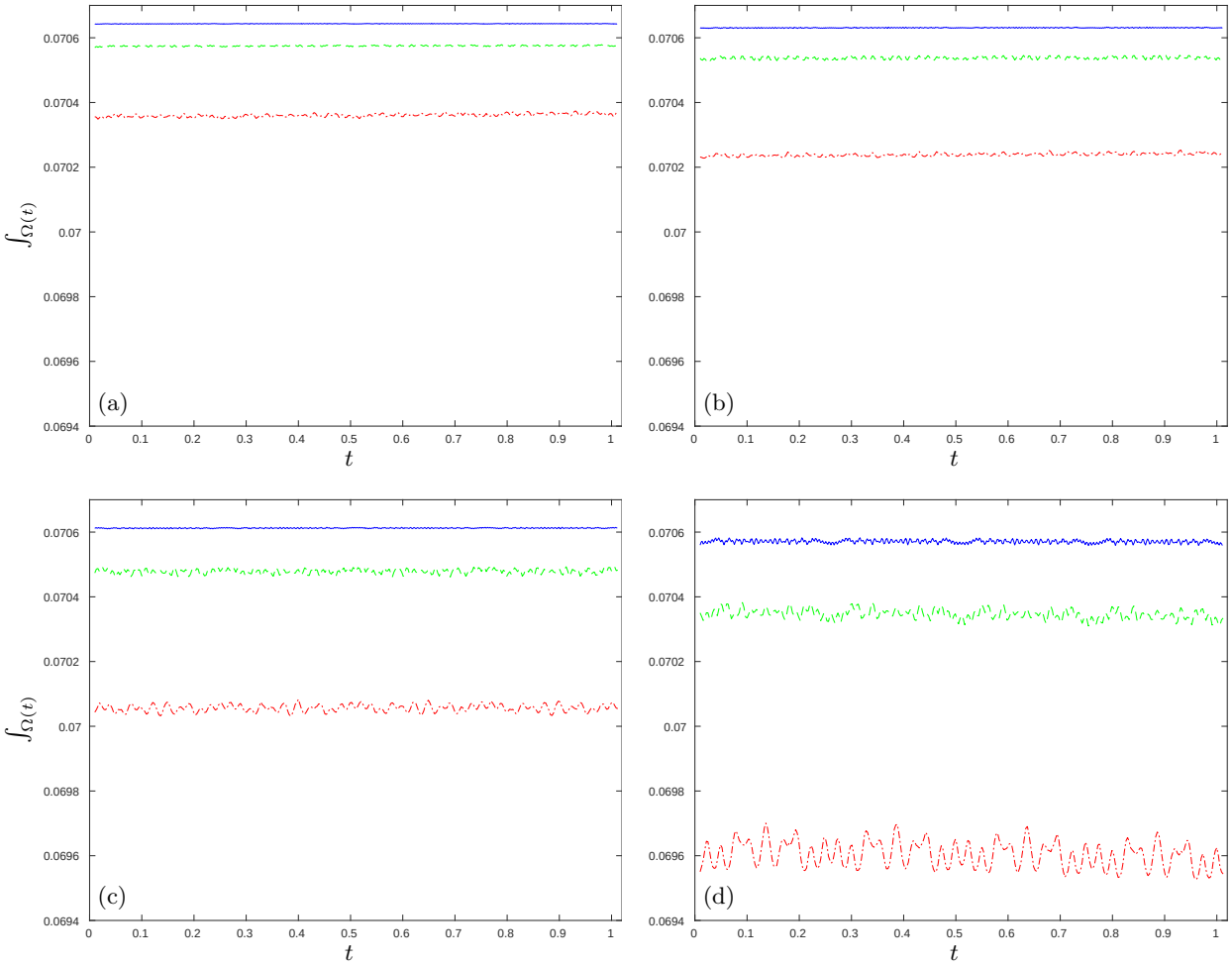

Figure 2.1: Volume $\int_{\Omega(t)}$ versus time period plots for a rotating circle problem for (a) $\delta = 1.8$, (b) $\delta = 1.5$, (c) $\delta = 1.2$, and (d) $\delta = 0.9$ with $\epsilon = 3.6 \times 10^{-2}$ (—·—), $\epsilon = 1.8 \times 10^{-2}$ (- - -), and $\epsilon = 0.9 \times 10^{-2}$ (——).

2.4.1 Benchmark I: Rotating Circle

In the first test, a circle of radius 0.15 being rotated around the center of a 1×1 domain with an offset equal to 0.25 from domain center has been studied. The evolution equation (2.11) is used with an advective velocity field, $\mathbf{u}(\mathbf{x})$, defined as

$$\mathbf{u}(\mathbf{x}) = (-2\pi y, 2\pi x), \tag{2.26}$$

where Cartesian coordinates x and y are used for simplicity of discussion.

To illustrate the sensitivity of the approach to mesh spacing compared to local grid resolution defined by Eq. (2.20), a set of tests on the rotating circle with different values of δ and ϵ have been performed. The results of the simulations are illustrated in Fig. 2.1, where the time history of the volume $\int_{\Omega(t)} d\mathbf{x}$ defined by the level set is shown for different parameters. These parameters and the corresponding volume conservation errors are listed in Table 2.1. As can be seen from the table, the volume conservation error is mostly dominated by local mesh resolution Δx, i.e., for the same interface thickness parameter ϵ the error is decreasing with the increase of δ. The iso-contours corresponding to ψ=0.05, 0.5, and 0.95 are shown for all cases in Fig. 2.2, which confirms a good performance of the method even for relatively large interface thickness. In the rest of this paper the simulations with $\delta = 0.9$ are performed.

Table 2.1: Sensitivity of volume conservation on model parameters for a circle rotation problem after one revolution.

Figure	δ	ϵ	Δx	Maximum deviation %
a	1.8	3.6×10^{-2}	2.0×10^{-2}	0.0191
b	1.8	1.8×10^{-2}	1.0×10^{-2}	0.0078
c	1.8	0.9×10^{-2}	0.5×10^{-2}	0.0025
d	1.5	3.6×10^{-2}	2.4×10^{-2}	0.0202
e	1.5	1.8×10^{-2}	1.2×10^{-2}	0.0123
f	1.5	0.9×10^{-2}	0.6×10^{-2}	0.0033
g	1.2	3.6×10^{-2}	3.0×10^{-2}	0.0383
h	1.2	1.8×10^{-2}	1.5×10^{-2}	0.0252
i	1.2	0.9×10^{-2}	0.75×10^{-2}	0.0038
j	0.9	3.6×10^{-2}	4.0×10^{-2}	0.1386
k	0.9	1.8×10^{-2}	2.0×10^{-2}	0.0530
l	0.9	0.9×10^{-2}	1.0×10^{-2}	0.0176

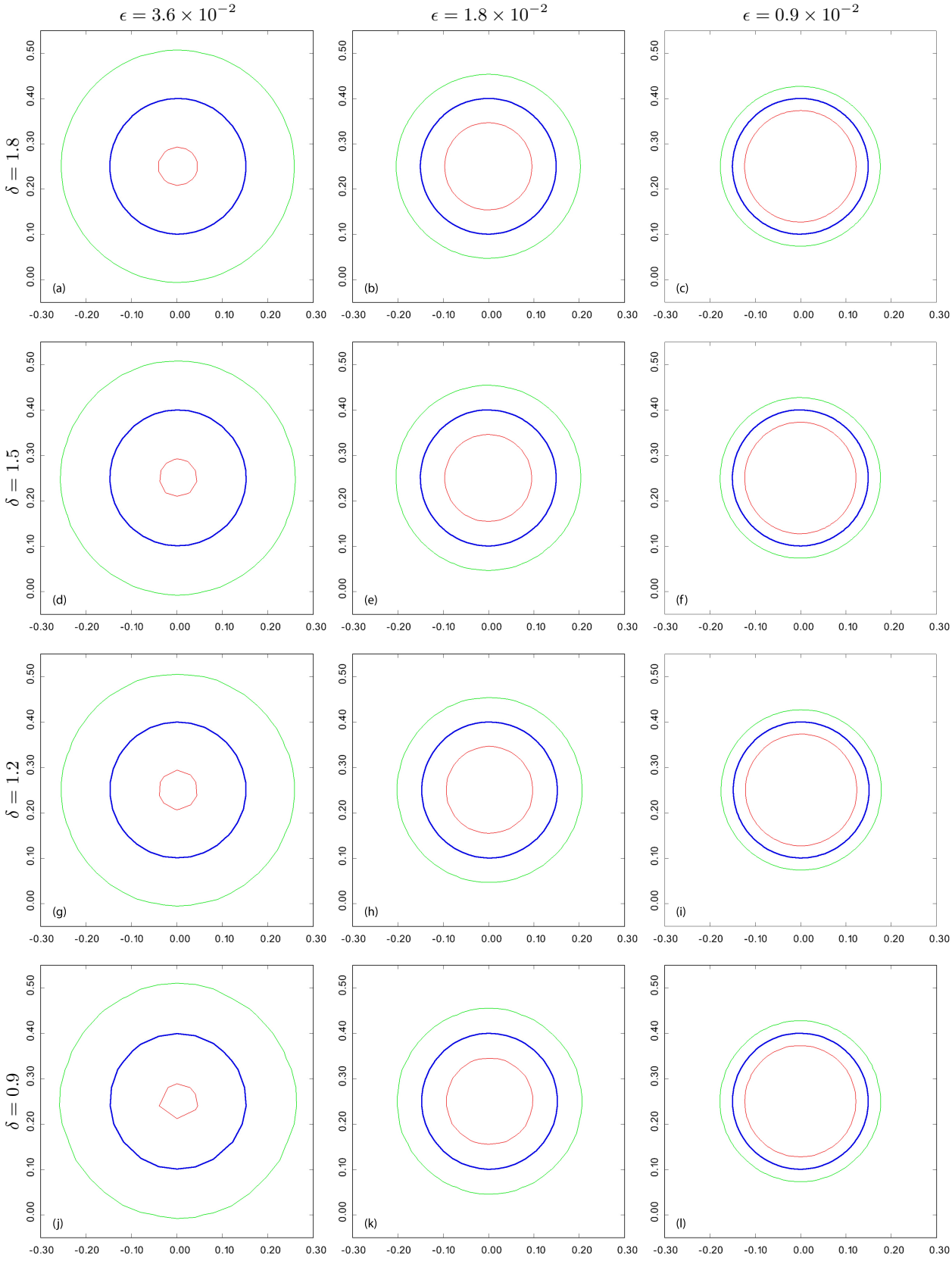

Figure 2.2: Iso-contours corresponding to ψ=0.05 (——), 0.5 (——), and 0.95 (——) after one revolution of a circle for different values of δ and ϵ (see Table 2.1 for corresponding values).

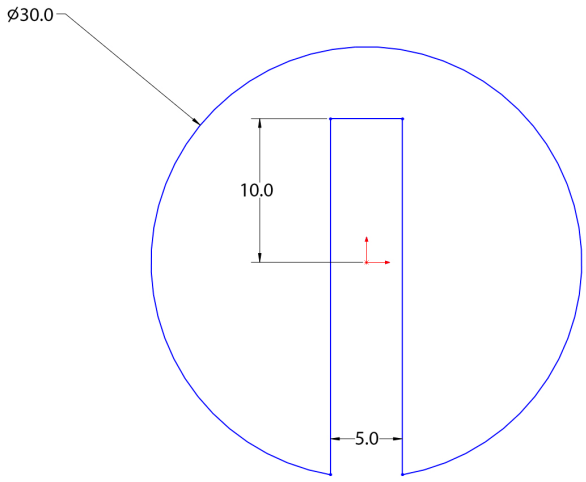

Figure 2.3: Schematic representation of disk.

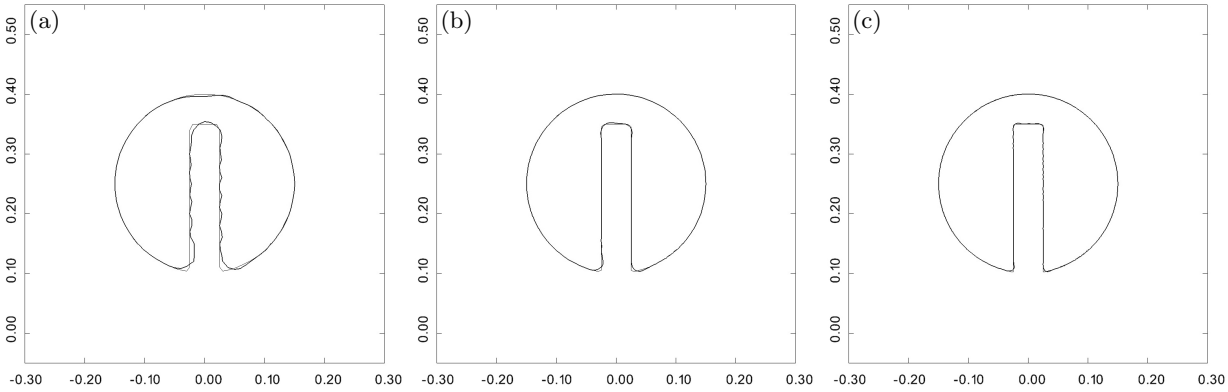

Figure 2.4: Contour plots for $\psi = 0.5$ for initial condition and after one revolution of the disk for different resolutions: (a) $\Delta x = 1 \times 10^{-2}$, (b) $\Delta x = 5 \times 10^{-3}$, and (c) $\Delta x = 2.5 \times 10^{-3}$ ($\delta = 0.9$).

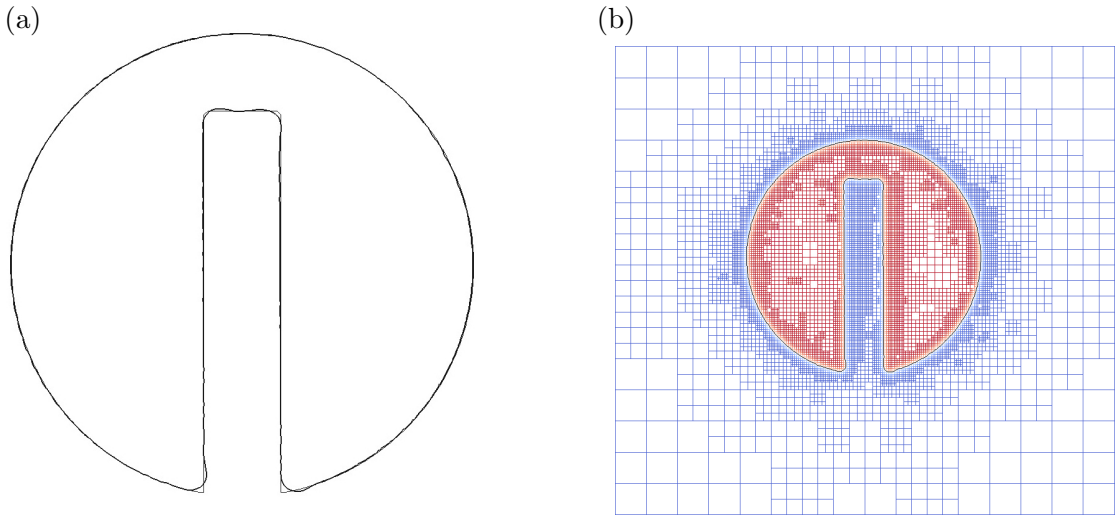

Figure 2.5: (a) Contour plots for $\psi = 0.5$ for initial condition and after third revolution of the disk and (b) an example of an adaptive mesh with the superimposed contour plot for $\psi = 0.5$ after one revolution with $\Delta x = 2.5 \times 10^{-3}$ and $\delta = 0.9$.

2.4.2 Benchmark II: Zalesak's Disk

The Zalesak's disk problem tests the ability of the proposed level-set method to accurately advect corners, sharp angles, and thin geometries. The Zalesak's disk problem consists of solid body rotation of a notched disk of radius 0.15 around center of a 1×1 domain in counterclockwise direction. Initially, the center of the disk is positioned in the middle of the horizontal axis with an offset of 0.25 units from domain center and the notch facing toward the rotation center. Figure 2.3 represents a schematic of the Zalesak's disk. The advective velocity field in this test is defined similar to the benchmark problem I, using equations (2.26). The results of the simulations for various grid sizes are shown in Fig. 2.4. The shape of the Zalesak's disk is captured well for all reported resolutions with increased accuracy for smaller mesh spacing. A comparison between the initial condition and the disk after three revolutions is shown in figure 2.5(a). Finally, the advantages of using adaptive mesh refinement in combination with stabilized conservative level set method is demonstrated in 2.5(b), where an adaptive mesh with the superimposed contour plot for $\psi = 0.5$ is shown.

2.4.3 Benchmark III: Vortex Drop

The vortex drop problems test the ability of the SCLS method to accurately resolve thin filaments which can occur in stretching and tearing flows. The first problem consists of an initially circular drop placed into a vortex with the oscillatory velocity field, $\mathbf{u}(\mathbf{x}, t)$, defined as

$$\mathbf{u}(\mathbf{x}, t) = \mathbf{u}_{\mathrm{st}}(\mathbf{x}) \cos\left(\frac{\pi t}{T}\right), \tag{2.27}$$

where T is the time period and the stationary velocity field, $\mathbf{u}_{\mathrm{st}}(\mathbf{x})$, is given by

$$\mathbf{u}_{\mathrm{st}}(\mathbf{x}) = \left(\cos^2(\pi x)\sin(2\pi y), -\cos^2(\pi y)\sin(2\pi x)\right). \tag{2.28}$$

At $t = 0.5T$, the velocity is reversed and counterclockwise rotation is applied on the stretched drop until it brings back the drop to its initial place at $t = T$.

Figure 2.6 shows the evolution of the drop at different times for different resolutions. Results show that the initial shape of the drop is preserved at $t = T$ for all the resolutions, with some noticeable oscillations at coarser resolution. In the second test, a vortex test without reversing the velocity field has been performed. To eliminate the time reversing effect, the stationary velocity field $\mathbf{u} = \mathbf{u}_{\mathrm{st}}(\mathbf{x})$ in Eq. (2.28) is used. As illustrated in figure 2.7, results show a continuous, uninterrupted strip after more than three rotation of the front of the drop around the domain center.

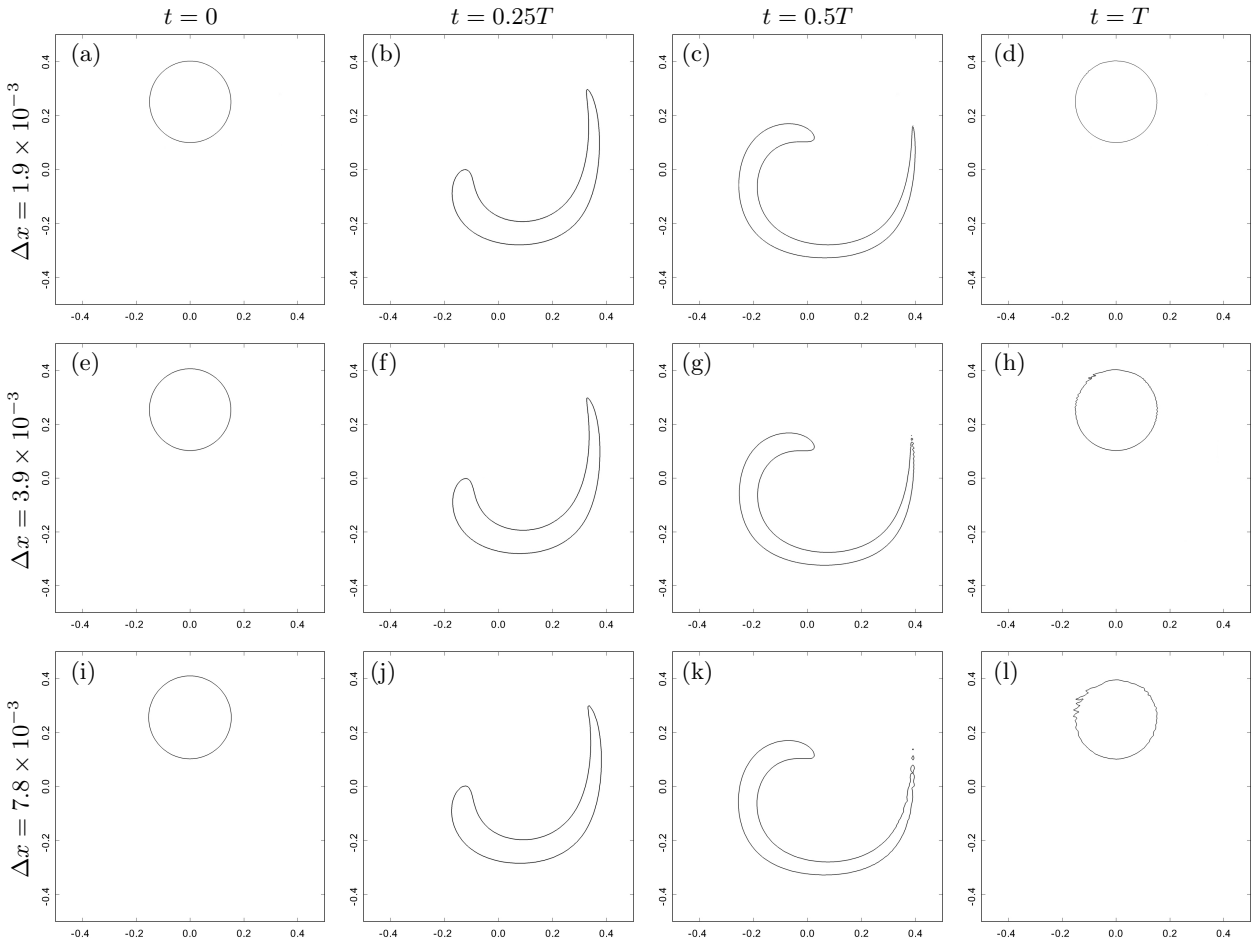

Figure 2.6: Evolution of contour plots for $\psi = 0.5$ for vortex drop problem at (a, e, i) $t = 0$, (b, f, j) $t = 0.25T$, (c, g, k) $t = 0.5T$, and (d, h, l) $t = T$ for $T = 3.4$ using SCLS method with different mesh sizes and $\delta = 0.9$.

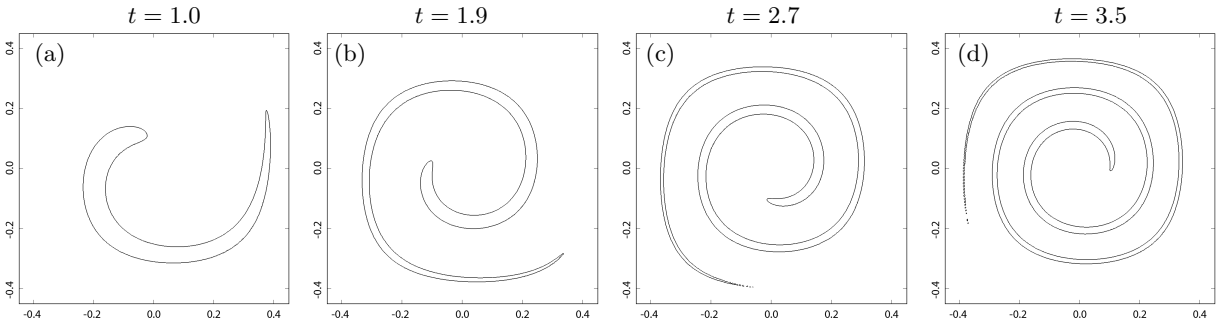

Figure 2.7: Evolution of the vortex without velocity reversing for $\Delta x = 1.9 \times 10^{-3}$ and $\delta = 0.9$ at different times.

Chapter 3

Conclusion and Future Work

The novel Stabilized Conservative Level Set method is presented in this work. The new formulation preserves the volume conservation properties. This approach, similar to the standard conservative level set method, utilizes compressive flux and diffusive terms only in normal direction with respect to the interface in the interfacial zone, while away from the interface the directional diffusion mechanism automatically switches to the isotropic diffusion. This is achieved by reformulating the reinitialization procedure based on a non-unit normal vector, whose magnitude diminishes in the regions far from the interface.

The resulting procedure is general, robust and stable, easy to implement, and does not require special topology treatments. The advantages of using the Stabilized Conservative Level Set method in combination with the adaptive wavelet-based mesh refinement methodology is also demonstrated. It was shown that the level set information are mostly important in the interface zone and in the far field its data are out of interest. Therefore, a finer resolution within the interface in combination with coarser resolution in the regions far from the interface would be just adequet to carry out the numerical tests. Hence, the integration of the two methodologies improves computational efficiency by adapting the mesh to adequately resolve interface regions without over-resolving solution fields away from the interface.

A number of benchmark numerical tests were performed to show the performance of the new level set method. In the first test, a circle disk was advected in a square domain with a rotational velocity field. The area versus time diagram was plotted for three different interface

thickness parameter. The results show that even for the coarsest resolution the volume of the disk was conserved at the end of the time period. Results also show that with decreasing the interface thickness parameter, the volume of the disk approaches the exact solution. It is noteworthy that the resolution was increased with decrease of the interface thickness parameter to ensure that the interface is resolved.

In the second benchmark test, a notched disk, known as Zalesaks disk was advected with a rotational velocity field to revolve counterclockwise around the center of a square domain. This test demonstrated the ability of the new method to accurately advect corners and sharp angles.

Lastly, the vortex drop test case was performed. In this test, first the circle was advected in a vortex velocity field until half period to show the performance of the method with resolving thin filements. Then, the velocity field was reversed to bring the vortex back into the drop shape. Results showed that the shape and volume of the circle was preserved very well at the end of the time period.

In conclusion, the numerical results demonstrate the ability of the new level set method to accurately advect corners, sharp angles, and resolve thin filaments, while preserving excellent conservation properties of the conservative level set method.

Future works include investigating immiscible compressible viscous fluid flows using stabilized conservative level set method to track the fluid interface. Immiscible fluid flows are essentially consist of fluids which do not form a homogeneous phase when mixed together. The immiscible flows are governed by the continuity, momentum, and energy equations. A front tracking method needs to accompany the flow equations to ensure a distinction between the volume occupied by each fluid.

Bibliography

[1] F. Avellan and M. Farhat. Shock pressure generated by cavitation vortex collapse. In 16th Aerospace Sciences Meeting, 88, pages 119–125. ASME Winter Annual Meeting, 1989.

[2] A. Bateni, S. S. Susnar, A. Amirfazli, and A. W. Neumann. Development of a new methodology to study drop shape and surface tension in electric fields. Langmuir, 20:7589–7597, 2004.

[3] G. Beylkin. Wavelets and fast numerical algorithms. In Proceedings of symposia in Applied Mathematics. American Mathematics Society.

[4] C. E. Brennen. Cavitation and Bubble Dynamics. Oxford University Press, London, 1995.

[5] H. Chen, X. Li, and M. Wan. The inception of cavitation bubble clouds induced by high-intensity focused ultrasound. Ultrasonics, 44:e427e429, 2006.

[6] G. De Stefano and O. V. Vasilyev. Perfect modeling framework for dynamic SGS model testing in large eddy simulation. Theor. Comp. Fluid Dyn., 18(1):27–41, 2004.

[7] L. Debnath. Wavelet Transforms and their application. Birkhuser, Boston, 2002.

[8] O. Desjardins, V. Moureau, and H. Pitsch. An accurate conservative level set/ghost fluid method for simulating turbulent atomization. J. Comput. Phys., 227:8395–8416, 2008.

[9] W. S. Edwards, L. S. Tuckerman, R. A. Friesner, and D. C. Sorensen. Krylov methods for the incompressible Navier–Stokes equations. J. Comp. Phys., 110:82–102, 1994.

[10] D. Enright, R. Fedkiw, J. Ferziger, and I. Mitchell. A hybrid particle level set method for improved interface capturing. J. Comput. Phys., 183:83–116, 2002.

[11] M. Farge. Wavelet transforms and their application to turbulence. Annu. Rev. Fluid Mech., 24:395–457, 1992.

[12] M. Gharib and P. Derango. A liquid film (soap film) tunnel to study two-dimensional laminar and turbulent shear flows. Physica D: Nonlinear Phenomena, 37:406–416, 1989.

[13] A. Grossmann and J. Morlet. Decomposition of hardy functions into square integrable wavelets of constant shape. SIAM J. Math. Anal., 15:723–736, 1984.

[14] B. B. Hubbard. The World According to Wavelets: The Story of a Mathematical Technique in the Making. A K Peters, Wellesley, 2 edition, 1998.

[15] D. Knight, H. Yan, A. G. Panaras, and A. Zheltovodov. Advances in CFD prediction of shock wave turbulent boundary layer interactions. Progress in Aerospace Sciences, 39:Progress in Aerospace Sciences, 203.

[16] R. B. Medvitz, R. F. Kunz, J. W. Lindau, A. M. Yocum, and L. L. pauley. Movement of location of tip vortex cavitation along blade edge due to reduction of flow rate in an axial pump. Int. J. of Mechanical and Aerospace Eng., 6:191–195, 2012.

[17] A. Nejadmalayeri, A. Vezolainen, E. Brown-Dymkoski, and O. V. Vasilyev. Parallel adaptive wavelet collocation method for pdes. J. Comput. Phys., 298:237–253, 2015.

[18] Alireza Nejadmalayeri, Alexei Vezolainen, Eric Brown-Dymkoski, and Oleg V. Vasilyev. Parallel adaptive wavelet collocation method for PDEs. J. Comp. Phys., 298:237–253, 2015.

[19] E. Olsson and G. Kreiss. A conservative level set method for two phase flow. J. Comput. Phys., 210:225–246, 2005.

[20] E. Olsson, G. Kreiss, and S. Zahedi. A conservative level set method for two phase flow ii. J. Comput. Phys., 225:785–807, 2007.

[21] Z. Qin, K. Delaney A. Riaz, and E. Balaras. Topology preserving advection of implicit interfaces on cartesian grids. J. Comput. Phys., 290:219–238, 2015.

[22] S. M. Reckinger, O. V. Vasilyev, and B. Fox-Kemper. Adaptive wavelet collocation method on the shallow water model. J. Comput. Phys., 271:342–359, 2014.

[23] G. Russo and P. Smereka. A remark on computing distance functions. J. Comput. Phys., 163:51–67, 2000.

[24] K. Schneider and O. V. Vasilyev. Wavelet methods in computational fluid dynamics. Annu. Rev. Fluid Mech., 42:473–503, 2010.

[25] J. A. Sethian. An analysis of flame propagation. PhD thesis, University of California, Berkley, 1982.

[26] J. A. Sethian. Level Set Methods and Fast Marching Methods: Evolving interfaces in computational geometry, fluid mechanics, computer vision, and materials science. Cambridge University Press, New York, 2 edition, 1999.

[27] M. T. Shervani-Tabar. Computer study of a cavity bubble near a rigid boundary, a free surface, and a compliant wall. PhD thesis, University of Wollongong, 1995.

[28] M. T. Shervani-Tabar, A. Abdullah, and M. R. Shabgard. Numerical study on the dynamics of an electrical discharge generated bubble in edm. Engineering Analysis with Boundary Elements, 30:503–514, 2006.

[29] M. T. Shervani-Tabar and N. Shervani-Tabar. Movement of location of tip vortex cavitation along blade edge due to reduction of flow rate in an axial pump. Int. J. of Mechanical and Aerospace Eng., 6:191–195, 2012.

[30] R. K. Shukla, C. Pantano, and J. B. Freund. An interface capturing method for the simulation of multi-phase compressible flows. J. Comput. Phys., 229:74117439, 2010.

[31] G. Strang and T. Nguyen. Wavelets and Filter Banks. Wellesley-Cambridge Press, Wellesley, 1 edition, 1997.

[32] M. Sussman and E. Fatemi. An efficient, interface-preserving level set redistancing algorithm and its application to interfacial incompressible fluid flow. SIAM J. Sci. Comput., 20:1165–1191, 1999.

[33] M Sussman, P Smereka, and S Osher. A level set approach for computing solutions to incompressible 2-phase flow. J. Comp. Phys., 114(1):146–159, 1994.

[34] W. Sweldens. The lifting scheme: A construction of second generation wavelets. SIAM J. Math. Anal., 29(2):511–546, 1998.

[35] Joe F. Thompson, B. K. Soni, and N. P. Weatherill, editors. Handbook of grid generation. CRC Press, Boca Raton, London, New York, 1999.

[36] O. V. Vasilyev. Solving multi-dimensional evolution problems with localized structures using second generation wavelets. International Journal of Computational Fluid Dynamics, 17(2):151–168, 2003.

[37] O. V. Vasilyev and C. Bowman. Second-generation wavelet collocation method for the solution of partial differential equations. J. Comput. Phys., 165:660693, 2000.

[38] O. V. Vasilyev and N. K. -R. Kevlahan. Hybrid wavelet collocation - Brinkman penalization method for complex geometry flows. Int. J. Numerical Methods in Fluids, 40:531–538, 2002.

[39] O. V. Vasilyev and N. K. -R Kevlahan. An adaptive multilevel wavelet collocation method for elliptic problems. J. Comp. Phys., 206(2):412–431, 2005.

[40] L. Zhao, X. Bai, T. Li, and J. J. R. Williams. Improved conservative level set method. Int. J. Numer. Meth. Fluids, 75:575–590, 2014.

[41] W. Zhao, L. Zhang, and X. Shao. Numerical simulation of cavitation flow under high pressure and temperature. Journal of Hydrodynamics, 23:289–294, 2011.